Comparative semi-empirical and *ab initio* atomic structure calculations in Yb-like tungsten W^{4+}

2012 J. Phys. B: At. Mol. Opt. Phys. 45 065001

(http://iopscience.iop.org/0953-4075/45/6/065001)

J. Phys. B: At. Mol. Opt. Phys. **45** (2012) 065001 (11pp) doi:10.1088/0953-4075/45/6/065001

Comparative semi-empirical and *ab initio* atomic structure calculations in Yb-like tungsten W^{4+}

S Enzonga Yoca[1], P Quinet[2,3], P Palmeri[2] and É Biémont[2,3]

[1] Département de Physique, Faculté des Sciences, Université Marien Ngouabi, BP 69 Brazzaville, Congo
[2] Astrophysique et Spectroscopie, Université de Mons—UMONS, B-7000 Mons, Belgium
[3] IPNAS, Université de Liège, B15 Sart Tilman, B-4000 Liège, Belgium

E-mail: quinet@umons.ac.be

Received 26 December 2011, in final form 6 February 2012
Published 6 March 2012
Online at stacks.iop.org/JPhysB/45/065001

Abstract
In this paper, we report on extensive calculations of radiative data in Yb-like tungsten ion using several independent atomic structure methods, i.e. the relativistic Hartree–Fock approach, the flexible atomic code and the multiconfiguration Dirac–Fock method. This multi-platform approach allowed us to check the consistency of our results. Advantages and shortcomings of semi-empirical and *ab initio* methods for atomic structure calculations in such a complex heavy ion are also discussed in detail. A new set of transition probabilities and oscillator strengths is reported for electric dipole lines together with magnetic dipole and electric quadrupole lines in this ion of interest for fusion plasma diagnostics.

1. Introduction

As mentioned in many previous papers (see e.g. Federici *et al* 2001, Neu *et al* 2005, Pospieszczyk 2006, Skinner 2008, 2009), the use of tungsten as a plasma-facing material in future magnetic fusion reactors, such as ITER, requires the knowledge of the atomic structure and radiative properties of almost each ionization stage of this element. Recently, we have reported spectroscopic data for neutral to moderately ionized tungsten. More precisely, transition probabilities were calculated for a large number of transitions in W I (Quinet *et al* 2011), W II (Nilsson *et al* 2008), W III (Palmeri *et al* 2008), W IV (Enzonga Yoca *et al* 2012a) and W VI (Enzonga Yoca *et al* 2012b). In these studies, the relativistic Hartree–Fock (HFR) method including core-polarization effects (HFR+CPOL) was combined with a semi-empirical process minimizing the discrepancies between calculated and available experimental energy levels. In all cases, the accuracy of this approach was assessed through detailed comparisons with experimental radiative lifetimes measured with the time-resolved laser-induced fluorescence (TR-LIF) technique (W I, W II, W III), with branching fractions deduced from line intensity ratios measured on high-resolution Fourier transform spectra (W I) or with transition probabilities obtained using different theoretical methods (W IV, W VI). Furthermore, critically evaluated transition rates available in the literature for allowed electric dipole lines together with a new set of computed *A*-values for forbidden lines were reported in a recent paper for W I, W II and W III (Quinet *et al* 2010).

In order to complete these investigations, this work is focused on quadruply ionized tungsten, W V. This ion is the third member of the ytterbium isoelectronic sequence (after Hf III and Ta IV) having the ground configuration $5s^25p^65d^2$, while the first two members of the sequence, Yb I and Lu II, have the ground configuration $5s^25p^66s^2$. In their compilation on spectroscopic data of tungsten ions, Kramida and Shirai (2009) reported, for Yb-like tungsten, 193 lines from 39 to 219 nm and 59 experimental energy levels belonging to $5d^2$, 5d6s, 5d6p, 6s6p, 5d5f and 5d7p configurations. This compilation was based on the work of Meijer (1986) who observed the W V spectrum in the 63–219 nm wavelength range by using a sliding-spark light source and on the works of Churilov *et al* (1996) and Kildiyarova *et al* (1996) who extended the identifications to the region 39–57 nm using similar light sources.

To our knowledge, the only radiative rates available in W V were published by Safronova and Safronova (2010) who

used the relativistic many-body perturbation theory (RMBPT) to compute oscillator strengths for 28 lines depopulating the levels belonging to the 5d6p configuration. In this paper, we report on extensive calculations of transition probabilities using several independent atomic structure methods, i.e. HFR approach, the flexible atomic code (FAC) and the multiconfiguration Dirac–Fock (MCDF) method. This multi-platform approach allowed us not only to check the consistency of our results but also to study the advantages and shortcomings of semi-empirical and *ab initio* methods for a complex heavy ion such as Yb-like tungsten.

2. Computational methods

2.1. Relativistic Hartree–Fock (HFR)

In the first step, we used the HFR approach (Cowan 1981) in which we have incorporated CPOL effects by means of a model potential and a correction to the dipole operator (HFR+CPOL; see e.g. Quinet *et al* 1999). In a previous work on the isoelectronic ion Hf III (Malcheva *et al* 2009), excellent agreement was obtained between HFR+CPOL lifetimes and the accurate experimental values measured for 5d6p and 6s6p states by TR-LIF spectroscopy. We have adopted the same physical model here considering a set of 45 configurations: $5d^2 + 5d6s + 5d7s + 5d6d + 5d7d + 6s^2 + 6s6d + 6s7d + 6s7s + 6p^2 + 6p7p + 6p5f + 6p6f + 6p7f + 6d^2 + 6d7s + 6d7d + 7s^2 + 7p^2 + 7s7d + 7p5f + 7p6f + 7p7f$ (even parity) and $5d6p + 5d7p + 5d5f + 5d6f + 5d7f + 6s6p + 6s7p + 6s5f + 6s6f + 6s7f + 6p6d + 6p7d + 6p7s + 6d7p + 6d5f + 6d6f + 6d7f + 7s5f + 7s6f + 7s7f + 7s7p + 7p7d$ (odd parity). For the CPOL corrections, we considered a $4f^{14}5s^25p^6$ erbium-like core surrounded by two valence electrons. The adopted dipole polarizability was $\alpha_d = 2.50\ a_0^3$ which corresponds to a W^{6+} ionic core and was found by extrapolating the values of α_d published by Fraga *et al* (1976) along the erbium isoelectronic sequence for Tm^+, Yb^{2+}, Lu^{3+} and Hf^{4+}. The cut-off radius used was the HFR mean radius of the outermost core orbital 5p, i.e. $r_c = 1.20\ a_0$. To optimize the calculation of oscillator strengths, the HFR+CPOL method was combined with a semi-empirical fitting of the radial parameters minimizing the discrepancies between the calculated energies and the experimental values compiled by Kramida and Shirai (2009) for the $5d^2$, 5d6s, 5d6p, 6s6p, 5d5f and 5d7p configurations. The mean deviations of the fits were found to be 20 cm^{-1} for the even parity and 132 cm^{-1} for the odd parity.

In the second HFR model (referred to as HFR(CV)), we restricted the intravalence correlation to $n = 6$ and $l = 3$ but we explicitly considered core-valence correlation from $5d^2$, 5d6s, 5d6p and 6s6p by including some configurations with a single excitation from 5s and 5p core orbitals. More precisely, in this model the following interacting configurations were included: $5d^2 + 5d6s + 5d6d + 6s^2 + 6s6d + 6p^2 + 6p5f + 6p6f + 6d^2 + 5p^55d^26p + 5p^55d6s6p + 5s5p^65d^3 + 5s5p^65d^26s + 5s5p^65d6s^2$ (even parity) and $5d6p + 5d5f + 5d6f + 6s6p + 6s5f + 6s6f + 6p6d + 6d5f + 6d6f + 5p^55d^3 + 5p^55d^26s + 5p^55d6s^2 + 5s5p^65d^26p + 5s5p^65d6s6p$ (odd parity). It was verified that other two-valence electron configurations, such as $5f^2$ or $6f^2$, had a negligible influence on the spectroscopic configurations of interest. Here also, a semi-empirical adjustment of the radial parameters was performed for $5d^2$, 5d6s, 5d6p, 6s6p and 5d5f configurations giving rise to average differences between calculated and experimental levels of 20 and 135 cm^{-1} for even and odd parities, respectively.

2.2. Flexible atomic code (FAC)

Another theoretical method used in our work was the one implemented in the FAC code which uses a fully relativistic *ab initio* approach based on the Dirac equation (Gu 2003). Here, the following configurations were retained in the configuration-interaction expansion when diagonalizing the multi-electron Dirac–Coulomb–Breit Hamiltonian: $5d^2$, 5d6s, 5d6d, $6s^2$, 6s6d, $6p^2$, 6p5f, 6p6f, $6d^2$, 5d6p, 5d5f, 5d6f, 6s6p, 6s5f, 6s6f, 6p6d, 6d5f, 6d6f for the valence–valence correlations, and $5s^25p^55d^3$, $5s^25p^55d^26s$, $5s^25p^55d^26p$, $5s^25p^55d6s^2$, $5s^25p^55d6s6p$, $5s5p^65d^3$, $5s5p^65d^26s$, $5s5p^65d^26p$, $5s5p^65d6s^2$ and $5s5p^65d6s6p$ for the core–valence correlations. The set of interacting configurations was thus exactly the same as the one used in the HFR(CV) model described above. The one-electron spin–orbitals were obtained by solving the self-consistent Dirac–Fock–Slater radial equations for a local central potential minimizing the average energy of a mean configuration built from $5d^2 + 5d6s + 5d6p$ spectroscopic configurations. Note that optimizing only on the ground configuration deteriorates the agreement with the experimental energies by a factor of about 2 due to the neglect of 5d relaxation. The Breit interaction was applied up to $n = 6$, while higher order relativistic corrections, like the vacuum polarization effect, were considered by the addition of an Uehling-type radial potential (Uehling 1935) in the calculation of the spin–orbitals. In the calculation of the oscillator strengths, the transition energies were replaced by the experimental values taken from Kramida and Shirai (2009).

2.3. Multiconfiguration Dirac–Fock (MCDF)

Finally, we performed a fully relativistic *ab initio* MCDF calculation of transition rates in W V using the latest version of the General-purpose Relativistic Atomic Structure Package (GRASP) developed by Norrington (2009) from the MCDF original code of Grant and co-workers (Grant *et al* 1980, McKenzie *et al* 1980) and improved by Dyall *et al* (1989). The computations were done with the extended average level option, introducing the configurations $5d^2 + 5d6s + 5d6d + 6s^2 + 6p^2 + 6d^2 + 5p^55d^26p + 5p^55d6s6p + 5s5p^65d^3 + 5s5p^65d^26s + 5s5p^65d6s^2$ (even parity) and $5d6p + 6s6p + 5p^55d^3 + 5p^55d^26s + 5p^55d6s^2 + 5s5p^65d^26p + 5s5p^65d6s6p$ (odd parity) and including transverse Breit and quantum electrodynamics corrections such as those due to self-energy and vacuum polarization effects using the routines developed by McKenzie *et al* (1980). In these routines, the leading correction to the Coulomb repulsion between electrons in quantum electrodynamics is considered as a

Table 1. Experimental and calculated energy levels in W V.

Configuration	Level	E_{exp}[a] (cm^{-1})	E_{calc}[b] (cm^{-1})	*LS*-composition[b]
Even parity				
$5d^2$	$^3F_2$	0.0	0	90% $5d^2\ ^3F$ + 10% $5d^2\ ^1D$
$5d^2$	$^3F_3$	6244.7	6236	100% $5d^2\ ^3F$
$5d^2$	$^3F_4$	11 519.4	11 468	91% $5d^2\ ^3F$ + 9% $5d^2\ ^1G$
$5d^2$	$^3P_0$	12 838.7	12 776	93% $5d^2\ ^3P$ + 7% $5d^2\ ^1S$
$5d^2$	$^1D_2$	13 741.5	13 721	56% $5d^2\ ^1D$ + 34% $5d^2\ ^3P$ + 9% $5d^2\ ^3F$
$5d^2$	$^3P_1$	16 330.6	16 351	100% $5d^2\ ^3P$
$5d^2$	$^1G_4$	22 345.8	22 330	91% $5d^2\ ^1G$ + 9% $5d^2\ ^3F$
$5d^2$	$^3P_2$	22 615.4	22 599	65% $5d^2\ ^3P$ + 32% $5d^2\ ^1D$
$5d^2$	$^1S_0$	43 110.1	43 094	92% $5d^2\ ^1S$ + 7% $5d^2\ ^3P$
5d6s	$^3D_1$	58 514.2	58 448	100% 5d6s ^3D
5d6s	$^3D_2$	60 295.5	60 331	89% 5d6s ^3D + 11% ^1D
5d6s	$^3D_3$	66 657.7	66 638	100% 5d6s ^3D
5d6s	$^1D_2$	72 958.7	72 933	86% 5d6s ^1D + 11% 5d6s ^3D
Odd parity				
5d6p	$^3F^\circ_2$	118 662.8	118 887	69% 5d6p $^3F^\circ$ + 26% 5d6p $^1D^\circ$
5d6p	$^3D^\circ_1$	122 325.8	121 994	71% 5d6p $^3D^\circ$ + 19% 5d6p $^1P^\circ$ + 10% 5d6p $^3P^\circ$
5d6p	$^3D^\circ_2$	128 997.1	129 135	49% 5d6p $^3D^\circ$ + 27% 5d6p $^3P^\circ$ + 20% 5d6p $^1D^\circ$
5d6p	$^3F^\circ_3$	129 479.5	129 348	68% 5d6p $^3F^\circ$ + 22% 5d6p $^3D^\circ$ + 10% 5d6p $^1F^\circ$
5d6p	$^1D^\circ_2$	133 430.0	133 489	40% 5d6p $^3D^\circ$ + 31% 5d6p $^1D^\circ$ + 26% 5d6p $^3F^\circ$
5d6p	$^3D^\circ_3$	136 887.8	136 790	43% 5d6p $^3D^\circ$ + 31% 5d6p $^3F^\circ$ + 25% 5d6p $^1F^\circ$
5d6p	$^3P^\circ_1$	137 709.3	137 761	62% 5d6p $^3P^\circ$ + 24% 5d6p $^3D^\circ$ + 13% 5d6p $^1P^\circ$
5d6p	$^3P^\circ_0$	139 252.1	139 218	99% 5d6p $^3P^\circ$
5d6p	$^3F^\circ_4$	142 907.9	142 801	100% 5d6p $^3F^\circ$
5d6p	$^3P^\circ_2$	144 389.9	144 465	68% 5d6p $^3P^\circ$ + 23% 5d6p $^1D^\circ$ + 7% 5d6p $^3D^\circ$
5d6p	$^1F^\circ_3$	145 767.9	145 764	63% 5d6p $^1F^\circ$ + 35% 5d6p $^3D^\circ$
5d6p	$^1P^\circ_1$	149 160.1	149 081	64% 5d6p $^1P^\circ$ + 28% 5d6p $^3P^\circ$ + 5% 5d6p $^3D^\circ$
6s6p	$^3P^\circ_0$	182 036.7	182 171	99% 6s6p $^3P^\circ$
6s6p	$^3P^\circ_1$	185 757.2	185 558	93% 6s6p $^3P^\circ$ + 6% 6s6p $^1P^\circ$
6s6p	$^3P^\circ_2$	198 108.2	198 102	99% 6s6p $^3P^\circ$
6s6p	$^1P^\circ_1$	215 212.7	215 199	83% 6s6p $^1P^\circ$ + 7% 5d5f $^1P^\circ$ + 6% 6s6p $^3P^\circ$
5d5f	$^1G^\circ_4$	227 536	227 317	46% 5d5f $^3H^\circ$ + 43% 5d5f $^1G^\circ$ + 9% 5d5f $^3F^\circ$
5d5f	$^3F^\circ_2$	228 702	228 640	75% 5d5f $^3F^\circ$ + 21% 5d5f $^1D^\circ$
5d5f	$^3H^\circ_4$	229 205	228 914	44% 5d5f $^3H^\circ$ + 23% 5d5f $^3G^\circ$ + 15% 5d5f $^1G^\circ$
5d5f	$^3F^\circ_3$	229 873	229 802	67% 5d5f $^3F^\circ$ + 25% 5d5f $^3G^\circ$ + 8% 5d5f $^3D^\circ$
5d5f	$^3H^\circ_5$	231 099	230 861	85% 5d5f $^3H^\circ$ + 8% 5d5f $^3G^\circ$ + 7% 5d5f $^1H^\circ$
5d5f	$^3G^\circ_3$	232 210	232 489	55% 5d5f $^3G^\circ$ + 24% 5d5f $^1F^\circ$ + 11% 5d5f $^3D^\circ$
5d5f	$^1D^\circ_2$	233 804	234 036	36% 5d5f $^1D^\circ$ + 35% 5d5f $^3P^\circ$ + 22% 5d5f $^3D^\circ$
5d5f	$^3F^\circ_4$	235 598	235 669	55% 5d5f $^3F^\circ$ + 37% 5d5f $^1G^\circ$ + 5% 5d5f $^3H^\circ$
5d5f	$^3D^\circ_1$	236 062	236 349	66% 5d5f $^3D^\circ$ + 21% 5d5f $^3P^\circ$ + 10% 5d5f $^1P^\circ$
5d5f	$^3H^\circ_6$		236 707	100% 5d5f $^3H^\circ$
5d5f	$^3G^\circ_4$	238 239	238 297	73% 5d5f $^3G^\circ$ + 17% 5d5f $^3F^\circ$ + 5% 5d5f $^1G^\circ$
5d5f	$^3D^\circ_2$	238 727	239 011	38% 5d5f $^1D^\circ$ + 30% 5d5f $^3D^\circ$ + 18% 5d5f $^3F^\circ$
5d5f	$^3D^\circ_3$	239 456	239 557	37% 5d5f $^3D^\circ$ + 23% 5d5f $^3F^\circ$ + 23% 5d5f $^1F^\circ$
5d5f	$^3G^\circ_5$	239 614	239 451	88% 5d5f $^3G^\circ$ + 10% 5d5f $^3H^\circ$
5d5f	$^1F^\circ_3$	242 636	242 664	51% 5d5f $^1F^\circ$ + 43% 5d5f $^3D^\circ$
5d5f	$^3P^\circ_2$	242 953	242 936	51% 5d5f $^3P^\circ$ + 42% 5d5f $^3D^\circ$ + 5% 5d5f $^1D^\circ$
5d5f	$^3P^\circ_1$	243 609	243 517	71% 5d5f $^3P^\circ$ + 26% 5d5f $^3D^\circ$
5d5f	$^3P^\circ_0$		243 969	98% 5d5f $^3P^\circ$
5d5f	$^1H^\circ_5$	247 139	246 516	91% 5d5f $^1H^\circ$ + 5% 5d5f $^3H^\circ$
5d5f	$^1P^\circ_1$	248 815	248 940	60% 5d5f $^1P^\circ$ + 15% 5d7p $^1P^\circ$ + 7% 5d5f $^3D^\circ$
5d7p	$^3F^\circ_2$	251 112	251 031	69% 5d7p $^3F^\circ$ + 24% 5d7p $^1D^\circ$
5d7p	$^3D^\circ_1$	252 797	252 853	71% 5d7p $^3D^\circ$ + 15% 5d5f $^1P^\circ$ + 7% 5d7p $^1P^\circ$
5d7p	$^3D^\circ_2$	256 688	256 669	58% 5d7p $^3D^\circ$ + 22% 5d7p $^3F^\circ$ + 17% 5d7p $^1D^\circ$
5d7p	$^3F^\circ_3$	257 895	257 694	71% 5d7p $^3F^\circ$ + 23% 5d7p $^1F^\circ$ + 5% 5d7p $^3D^\circ$
5d7p	$^3P^\circ_1$	258 778	258 830	70% 5d7p $^3P^\circ$ + 15% 5d7p $^3D^\circ$ + 11% 5d7p $^1P^\circ$
5d7p	$^3P^\circ_0$	259 100	259 154	99% 5d7p $^3P^\circ$
5d7p	$^1D^\circ_2$	260 035	260 106	33% 5d7p $^3D^\circ$ + 30% 5d7p $^1D^\circ$ + 30% 5d7p $^3P^\circ$
5d7p	$^1F^\circ_3$	260 388	260 244	40% 5d7p $^3D^\circ$ + 33% 5d7p $^1F^\circ$ + 25% 5d7p $^3F^\circ$
5d7p	$^3D^\circ_3$	265 733	265 871	54% 5d7p $^3D^\circ$ + 42% 5d7p $^1F^\circ$
5d7p	$^3F^\circ_4$	266 010	265 769	99% 5d7p $^3F^\circ$

Table 1. (Continued.)

Configuration	Level	E^{a}_{exp} (cm^{-1})	E^{b}_{calc} (cm^{-1})	*LS*-composition[b]
5d7p	$^3P^\circ_2$	266 271	266 274	65% 5d7p $^3P^\circ$ + 29% 5d7p $^1D^\circ$
5d7p	$^1P^\circ_1$	269 124	269 186	65% 5d7p $^1P^\circ$ + 23% 5d7p $^3P^\circ$ + 6% 5d7p $^3D^\circ$

[a] From Kramida and Shirai (2009).
[b] This work (HFR+CPOL).

Table 2. Comparison of energy levels (in cm^{-1}) computed using different methods with experimental values for $5d^2$, 5d6s, 5d6p and 6s6p configurations in W V. For the abbreviations, see the text.

Configuration	*LS*	*jj*	EXP[a]	HFR+CPOL[b]	HFR(CV)[b]	FAC[b]	MCDF[b]	RMBPT[c]
$5d^2$	$^3F_2$	$(3/2,3/2)_2$	0.0	0	0	0	0	0
$5d^2$	$^3F_3$	$(3/2,5/2)_3$	6244.7	6236	6235	6296	5436	6496
$5d^2$	$^3F_4$	$(3/2,5/2)_4$	11 519.4	11 468	11 462	11 916	10 484	12 116
$5d^2$	$^3P_0$	$(3/2,3/2)_0$	12 838.7	12 776	12 776	14 691	14 186	12 910
$5d^2$	$^1D_2$	$(3/2,5/2)_2$	13 741.5	13 721	13 713	14 909	14 159	13 890
$5d^2$	$^3P_1$	$(3/2,5/2)_1$	16 330.6	16 351	16 343	17 972	16 938	16 510
$5d^2$	$^1G_4$	$(5/2,5/2)_4$	22 345.8	22 330	22 328	24 965	23 729	22 062
$5d^2$	$^3P_2$	$(5/2,5/2)_2$	22 615.4	22 599	22 602	24 154	22 350	23 098
$5d^2$	$^1S_0$	$(5/2,5/2)_0$	43 110.1	43 094	43 090	49 140	47 030	42 696
5d6s	$^3D_1$	$(3/2,1/2)_1$	58 514.2	58 448	58 450	51 516	53 889	58 995
5d6s	$^3D_2$	$(3/2,1/2)_2$	60 295.5	60 331	60 323	53 599	55 827	60 856
5d6s	$^3D_3$	$(5/2,1/2)_3$	66 657.7	66 638	66 635	59 787	61 386	67 497
5d6s	$^1D_2$	$(5/2,1/2)_2$	72 958.7	72 933	72 931	68 463	69 821	73 228
5d6p	$^3F^\circ_2$	$(3/2,1/2)^\circ_2$	118 662.8	118 887	118 993	118 006	113 522	120 349
5d6p	$^3D^\circ_1$	$(3/2,1/2)^\circ_1$	122 325.8	121 994	121 990	121 561	117 646	124 248
5d6p	$^3D^\circ_2$	$(3/2,3/2)^\circ_2$	128 997.1	129 135	128 890	128 231	123 024	131 077
5d6p	$^3F^\circ_3$	$(3/2,3/2)^\circ_3$	129 479.5	129 348	129 477	129 237	124 154	131 589
5d6p	$^1D^\circ_2$	$(5/2,1/2)^\circ_2$	133 430.0	133 489	133 341	132 573	127 584	135 469
5d6p	$^3D^\circ_3$	$(5/2,1/2)^\circ_3$	136 887.8	136 790	136 866	136 288	131 658	139 302
5d6p	$^3P^\circ_1$	$(3/2,3/2)^\circ_1$	137 709.3	137 761	137 722	137 437	132 675	139 942
5d6p	$^3P^\circ_0$	$(3/2,3/2)^\circ_0$	139 252.1	139 218	139 179	139 215	134 207	141 521
5d6p	$^3F^\circ_4$	$(5/2,3/2)^\circ_4$	142 907.9	142 801	142 885	142 950	136 756	145 196
5d6p	$^3P^\circ_2$	$(5/2,3/2)^\circ_2$	144 389.9	144 465	144 203	144 226	138 276	146 689
5d6p	$^1F^\circ_3$	$(5/2,3/2)^\circ_3$	145 767.9	145 764	146 073	145 641	142 278	148 222
5d6p	$^1P^\circ_1$	$(5/2,3/2)^\circ_1$	149 160.1	149 081	149 086	149 546	144 157	151 643
6s6p	$^3P^\circ_0$	$(1/2,1/2)^\circ_0$	182 036.7	182 171	182 161	183 449	175 050	184 705
6s6p	$^3P^\circ_1$	$(1/2,1/2)^\circ_1$	185 757.2	185 558	185 566	187 576	179 349	188 644
6s6p	$^3P^\circ_2$	$(1/2,3/2)^\circ_2$	198 108.2	198 102	198 098	200 128	191 077	201 195
6s6p	$^1P^\circ_1$	$(1/2,3/2)^\circ_1$	215 212.7	215 199	215 199	219 281	218 433	215 620

[a] From Kramida and Shirai (2009).
[b] This work.
[c] From Safronova and Safronova (2010)

first perturbation using the transverse Breit operator given by Grant and McKenzie (1980), the second-order vacuum polarization corrections are evaluated using the prescription of Fullerton and Rinker (1976) and the self-energy contributions are estimated by interpolating the hydrogenic $n = 1, 2$ results of Mohr (1974, 1975) and by scaling to higher n states according to $1/n^3$. In addition, the MCDF oscillator strengths were corrected with transition energies deduced from experimentally known energy levels taken from the compilation of Kramida and Shirai (2009).

3. Results and discussion

3.1. Energy levels

Calculated energy levels obtained with the HFR+CPOL method are compared to available experimental values in table 1. The largest *LS*-components of the wavefunctions are also reported in that table. One can observe that many of these levels are strongly mixed, the average *LS*-purities being equal to 89% and 68% for even and odd parities, respectively. For comparison, it is interesting to note that the fully relativistic MCDF calculations gave average purities in *jj*-coupling equal to 84% for $5d^2$ + 5d6s and 88% for 5d6p. For these configurations, the correlation between *LS* and *jj* designations are given in table 2 together with a comparison between experimental energies and those obtained using different computational approaches. While, as expected and already mentioned above, the two semi-empirical HFR models are in excellent agreement with experiment, rather large discrepancies are observed, in some cases, when considering the *ab initio* methods for which the average deviations $\Delta E = |E_{exp} - E_{calc}|$ are of the order of 1376, 1882 and 3930 cm^{-1} for RMBPT, FAC and MCDF, respectively. However, it is worth

Table 3. Comparison of oscillator strengths for $5d^2$–5d6p and 5d6s–5d6p transitions in W V. For the abbreviations, see the text.

λ_{exp}[a]			log *gf*				
(nm)	Lower level	Upper level	HFR+CPOL[b]	HFR(CV)[b]	FAC[b]	MCDF[b]	RMBPT[c]
72.3876	$5d^2\ ^3F_3$	$5d6p\ ^3P^\circ_2$	−0.99	−1.02	−1.22	−1.05	−1.12
72.6162	$5d^2\ ^3F_2$	$5d6p\ ^3P^\circ_1$	−0.86	−0.90	−1.05	−0.96	−1.08
73.1725	$5d^2\ ^3F_3$	$5d6p\ ^3F^\circ_4$	−1.10	−1.11	−1.21	−1.17	−1.11
73.3560	$5d^2\ ^3P_0$	$5d6p\ ^1P^\circ_1$	−1.35	−1.36	−1.36	−1.32	−1.49
76.1103	$5d^2\ ^3F_4$	$5d6p\ ^3F^\circ_4$	0.02	0.01	−0.06	0.00	0.03
77.5212	$5d^2\ ^3F_2$	$5d6p\ ^3D^\circ_2$	−1.29	−1.27	−1.25	−1.06	−1.18
78.0884	$5d^2\ ^3P_1$	$5d6p\ ^3P^\circ_2$	−0.85	−0.85	−0.89	−0.82	−0.80
78.6254	$5d^2\ ^3F_3$	$5d6p\ ^1D^\circ_2$	−0.08	−0.09	−0.18	−0.05	−0.04
79.7645	$5d^2\ ^3F_4$	$5d6p\ ^3D^\circ_3$	0.25	0.25	0.18	0.31	0.29
80.0832	$5d^2\ ^3P_0$	$5d6p\ ^3P^\circ_1$	−0.97	−0.97	−1.03	−0.94	−0.87
81.0225	$5d^2\ ^1G_4$	$5d6p\ ^1F^\circ_3$	0.44	0.44	0.39	0.52	0.47
81.1460	$5d^2\ ^3F_3$	$5d6p\ ^3F^\circ_3$	−0.08	−0.09	−0.13	−0.06	−0.06
81.3528	$5d^2\ ^3P_1$	$5d6p\ ^3P^\circ_0$	−0.58	−0.58	−0.63	−0.55	−0.60
81.4653	$5d^2\ ^3F_3$	$5d6p\ ^3D^\circ_2$	−0.20	−0.20	−0.20	−0.18	−0.27
81.7492	$5d^2\ ^3F_2$	$5d6p\ ^3D^\circ_1$	−0.11	−0.12	−0.15	−0.06	−0.10
82.1188	$5d^2\ ^3P_2$	$5d6p\ ^3P^\circ_2$	0.08	0.07	0.03	0.10	0.10
82.3875	$5d^2\ ^3P_1$	$5d6p\ ^3P^\circ_1$	−0.67	−0.68	−0.73	−0.62	−0.68
82.9450	$5d^2\ ^1G_4$	$5d6p\ ^3F^\circ_4$	−1.03	−1.03	−1.17	−1.25	−1.31
85.3980	$5d^2\ ^3P_1$	$5d6p\ ^1D^\circ_2$	−1.72	−1.74	−1.98	−1.39	−1.63
87.3045	$5d^2\ ^1G_4$	$5d6p\ ^3D^\circ_3$	−0.55	−0.70	−0.69	−0.88	−0.93
118.9151	$5d6s\ ^3D_2$	$5d6p\ ^3P^\circ_2$	−0.48	−0.44	−0.36	−0.35	−0.33
123.8574	$5d6s\ ^3D_1$	$5d6p\ ^3P^\circ_0$	−0.47	−0.43	−0.43	−0.47	−0.49
126.2707	$5d6s\ ^3D_1$	$5d6p\ ^3P^\circ_1$	−0.13	−0.11	−0.14	−0.18	−0.24
126.4066	$5d6s\ ^3D_3$	$5d6p\ ^1F^\circ_3$	−0.07	−0.11	−0.16	−0.38	−0.45
130.5611	$5d6s\ ^3D_2$	$5d6p\ ^3D^\circ_3$	0.29	0.31	0.30	0.24	0.16
131.1465	$5d6s\ ^3D_3$	$5d6p\ ^3F^\circ_4$	0.52	0.54	0.54	0.52	0.49
133.4841	$5d6s\ ^3D_1$	$5d6p\ ^1D^\circ_2$	−0.01	0.02	0.03	0.01	−0.02
144.5413	$5d6s\ ^3D_2$	$5d6p\ ^3F^\circ_3$	−0.27	−0.25	−0.23	−0.16	−0.09

[a] From Kramida and Shirai (2009).
[b] This work.
[c] From Safronova and Safronova (2010).

Table 4. Influence of the level mixing on the calculated oscillator strength of the $5d6s\ ^3D_3$–$5d6p\ ^1F^\circ_3$ transition.

Method	Mixing of $5d6p\ ^1F^\circ_3$	log *gf*
HFR+CPOL	63% $^1F^\circ$ + 37% $^3D^\circ$	−0.07
	67% $^1F^\circ$ + 33% $^3D^\circ$	−0.14
	72% $^1F^\circ$ + 28% $^3D^\circ$	−0.20
	75% $^1F^\circ$ + 25% $^3D^\circ$	−0.26
	78% $^1F^\circ$ + 22% $^3D^\circ$	−0.31
	82% $^1F^\circ$ + 18% $^3D^\circ$	−0.38
MCDF	82% $^1F^\circ$ + 18% $^3D^\circ$	−0.38

Table 5. Influence of the level mixing on the calculated oscillator strength of the $5d^2\ ^1G_4$–$5d6p\ ^3F^\circ_4$ transition.

Method	Mixing of $5d^2\ ^1G_4$	log *gf*
HFR+CPOL	91% ^1G + 9% ^3F	−1.03
	92% ^1G + 8% ^3F	−1.09
	93% ^1G + 7% ^3F	−1.14
	94% ^1G + 6% ^3F	−1.24
MCDF	94% ^1G + 6% ^3F	−1.25

noting that the strongly mixed 5d6p odd-parity levels are much better reproduced with the FAC model ($\Delta E = 410\ \mathrm{cm}^{-1}$) than with the MCDF approach ($\Delta E = 5253\ \mathrm{cm}^{-1}$) or with the RMBPT calculations of Safronova and Safronova (2010) ($\Delta E = 2190\ \mathrm{cm}^{-1}$).

3.2. Electric dipole transitions

In table 3, we compare the oscillator strengths deduced from the HFR+CPOL, HFR(CV), FAC and MCDF calculations with those computed using the RMBPT method by Safronova and Safronova (2010) for $5d^2$–5d6p and 5d6s–5d6p transitions. These comparisons are also illustrated in figure 1. When looking into details, it is clearly seen that an overall good agreement is obtained between the different calculations for most of the lines. In particular, the HFR+CPOL and HFR(CV) results agree within a few per cent indicating that the core-polarization model potential included in the former approach allows for a realistic representation of the core–valence interactions explicitly considered in the latter model.

When comparing the HFR+CPOL f-values to other calculations, a slightly better agreement is found with FAC than with MCDF and RMBPT methods, although the mean relative deviations are found to be similar, i.e. Δgf(HFR+CPOL–FAC) = 15%, Δgf(HFR+CPOL–MCDF) = 21% and Δgf(HFR+CPOL–RMBPT) = 20%. It is also interesting to note that the FAC and MCDF oscillator strengths

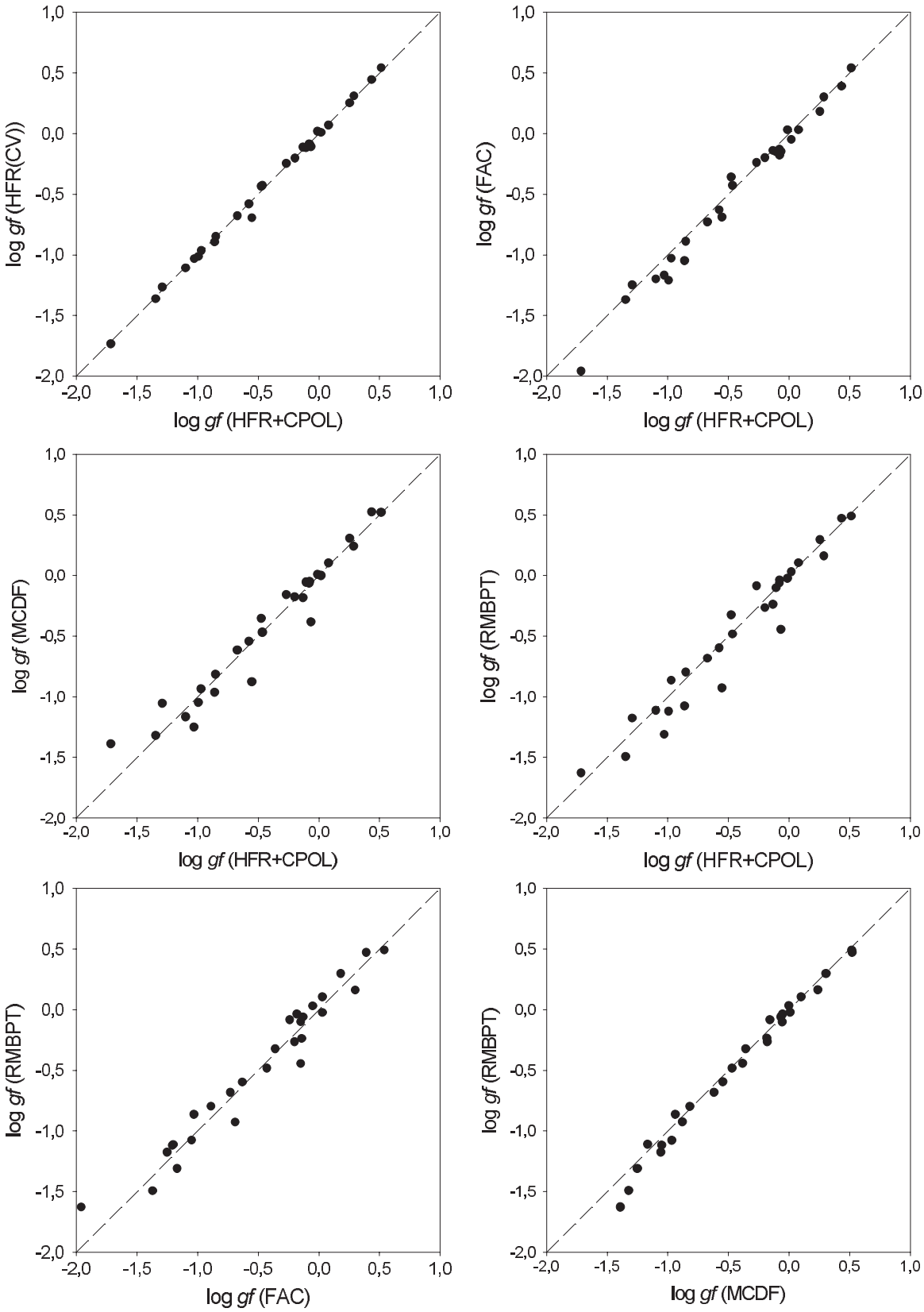

Figure 1. Comparison between oscillator strengths (log gf) obtained with different methods for $5d^2$–5d6p and 5d6s–5d6p transitions in W V. For the abbreviations, see the text.

Table 6. Influence of the level mixing on the calculated oscillator strength of the $5d^2\ ^1G_4$–$5d6p\ ^3D^\circ_3$ transition.

Method	Mixing of $5d^2\ ^1G_4$	Mixing of $5d6p\ ^3D^\circ_3$	log gf
HFR+CPOL	91% ^{1}G + 9% ^{3}F	43% ^{3}D° + 31% ^{3}F° + 25% ^{1}F°	−0.55
	92% ^{1}G + 8% ^{3}F	43% ^{3}D° + 31% ^{3}F° + 25% ^{1}F°	−0.52
	93% ^{1}G + 7% ^{3}F	43% ^{3}D° + 31% ^{3}F° + 25% ^{1}F°	−0.49
	94% ^{1}G + 6% ^{3}F	43% ^{3}D° + 31% ^{3}F° + 25% ^{1}F°	−0.44
	91% ^{1}G + 9% ^{3}F	47% ^{3}D° + 30% ^{3}F° + 22% ^{1}F°	−0.66
	91% ^{1}G + 9% ^{3}F	51% ^{3}D° + 29% ^{3}F° + 20% ^{1}F°	−0.78
	91% ^{1}G + 9% ^{3}F	54% ^{3}D° + 28% ^{3}F° + 17% ^{1}F°	−0.92
	91% ^{1}G + 9% ^{3}F	57% ^{3}D° + 27% ^{3}F° + 15% ^{1}F°	−1.06
	94% ^{1}G + 6% ^{3}F	57% ^{3}D° + 27% ^{3}F° + 15% ^{1}F°	−0.85
MCDF	94% ^{1}G + 6% ^{3}F	59% ^{3}D° + 28% ^{3}F° + 12% ^{1}F°	−0.88

agree within 25% and 13%, respectively, with RMBPT results of Safronova and Safronova (2010).

While the convergence of results using different approaches or physical models gives us confidence in the accuracy of the results obtained in this work, for a few lines the different methods do still give different results, up to a factor of 2. However, these situations are rather special, arising because of high sensitivity of f-values to the wavefunction mixings. Three examples of intercombination transitions will suffice to demonstrate the difficulty in obtaining accurate results in these situations:

(a) $5d6s\ ^3D_3$–$5d6p\ ^1F^\circ_3$. For this transition, the HFR+CPOL, HFR(CV) and FAC f-values are about a factor of 2 larger than the MCDF and RMBPT results. Since the spins of the two states are different, the transition is driven by the admixture of $5d6p\ ^3D^\circ_3$ in $5d6p\ ^1F^\circ_3$. In the *ab initio* MCDF calculation, the mixing was found to be 82% ^{1}F° + 18% ^{3}D°, while the corresponding mixing in the semi-empirical HFR+CPOL approach was found to be 63% + 37%. As illustrated in table 4, when modifying the HFR+CPOL wavefunctions (by slightly changing the numerical values of Slater integrals) to reproduce the MCDF mixing, excellent agreement is observed between the oscillator strengths.

(b) $5d^2\ ^1G_4$–$5d6p\ ^3F^\circ_4$. Here again, a large discrepancy is observed between HFR+CPOL and HFR(CV) results, on the one hand, and MCDF and RMBPT results, on the other hand. This intercombination line is driven by the $5d^2\ ^3F_4$ component in $5d^2\ ^1G_4$ state. Although this admixture is only of a few per cent, the small difference between the HFR+CPOL wavefunction (91% ^{1}G + 9% ^{3}F) and the MCDF one (94% ^{1}G + 6% ^{3}F) explains the discrepancy by a factor of 1.7 between the oscillator strengths as shown in table 5.

(c) $5d^2\ ^1G_4$–$5d6p\ ^3D^\circ_3$. In this case, the situation is even more complex since this transition is made possible by both the admixture of $5d^2\ ^3F_4$ in $5d^2\ ^1G_4$ and the admixture of $5d6p\ ^1F^\circ_3$ in $5d6p\ ^3D^\circ_3$. The sensitivity of the corresponding oscillator strength to the wavefunction compositions is shown in table 6. It is clearly seen that the oscillator strength is very sensitive to a small change (of a few per cent) in the wavefunction mixings of both the lower and upper states. However, good agreement is found when *LS*-coupling conditions are close to each other in both HFR+CPOL and MCDF methods.

These examples illustrate the high sensitivity of some transition rates to intermediate coupling and hence to level mixings which are expected to be better estimated when the calculated energy levels are closer to the experimental ones. For such particular situations, the semi-empirical HFR+CPOL and HFR(CV) approaches, allowing for an excellent representation of the W V atomic structure, are probably better adapted than *ab initio* methods which reproduce the experimental energies with a rather limited accuracy.

Transition probabilities and oscillator strengths computed using the semi-empirical HFR+CPOL model are listed in table 7 for a set of W V transitions between 39 and 179 nm with log $gf \geqslant -1$. A more comprehensive table is available in our DatabasE on SIxth Row Elements (DESIRE) at the following address: http://w3.umons.ac.be/astro/desire.shtml.

3.3. Forbidden transitions

Because they have radiative intensities which are often very sensitive to electron temperature and density, magnetic dipole (M1) and electric quadrupole (E2) transitions also play an important role in plasma diagnostics. Therefore, wavelengths and transition rates for such lines in various ionization stages of tungsten must be determined with high confidence. In table 8, we present transition probabilities computed with the HFR+CPOL model for selected forbidden lines involving levels of $5d^2$ and 5d6s even-parity configurations in W V. When the two types of radiation contribute to the intensity of a line then the sum of both A-values is given. It is worth mentioning that an overall good agreement was observed when comparing these transition probabilities with the FAC and MCDF values obtained in this work, in particular for the most intense lines. More precisely, it was found that the mean ratios $A_{\mathrm{HFR+CPOL}}/A_{\mathrm{FAC}}$ and $A_{\mathrm{HFR+CPOL}}/A_{\mathrm{MCDF}}$ were equal to 1.052 ± 0.066 and 0.949 ± 0.071 (for $A \geqslant 100\ \mathrm{s}^{-1}$), 1.161 ± 0.249 and 1.137 ± 0.362 (for $A \geqslant 10\ \mathrm{s}^{-1}$) and 1.120 ± 0.222 and 1.165 ± 0.359 (for $A \geqslant 2\ \mathrm{s}^{-1}$), where the uncertainty represents the standard deviation of the mean.

Table 7. Computed oscillator strengths (log gf) and transition probabilities (gA) in W V. Only allowed transitions for which log $gf \geqslant -1$ are listed. A(B) is written for A $\times$ 10^B.

	Lower level[a]		Upper level[a]			
λ^a(nm)	E (cm^{-1})	Designation	E (cm^{-1})	Designation	log gf^c	gA^c(s^{-1})
39.9295	6244.7	$5d^2\ ^3F_3$	256 688	$5d7p\ ^3D^\circ_2$	−0.92	5.02(09)
40.1824	11 519.4	$5d^2\ ^3F_4$	260 388	$5d7p\ ^1F^\circ_3$	−0.93	4.81(09)
41.0415	22 615.4	$5d^2\ ^3P_2$	266 271	$5d7p\ ^3P^\circ_2$	−0.85	5.56(09)
41.0869	22 345.8	$5d^2\ ^1G_4$	265 733	$5d7p\ ^3D^\circ_3$	−0.70	7.85(09)
42.4413[b]	11 519.4	$5d^2\ ^3F_4$	247 139	$5d5f\ ^1H^\circ_5$	−1.00	3.70(09)
42.8787	6244.7	$5d^2\ ^3F_3$	239 456	$5d5f\ ^3D^\circ_3$	−0.35	1.61(10)
43.0140[b]	6244.7	$5d^2\ ^3F_3$	238 727	$5d5f\ ^3D^\circ_2$	−0.88	4.74(09)
43.0643	0.0	$5d^2\ ^3F_2$	232 210	$5d5f\ ^3G^\circ_3$	0.37	8.37(10)
43.1045	6244.7	$5d^2\ ^3F_3$	238 239	$5d5f\ ^3G^\circ_4$	0.45	1.01(11)
43.5012	0.0	$5d^2\ ^3F_2$	229 873	$5d5f\ ^3F^\circ_3$	0.06	4.07(10)
43.5033[b]	13 741.5	$5d^2\ ^1D_2$	243 609	$5d5f\ ^3P^\circ_1$	−0.72	6.76(09)
43.6001	6244.7	$5d^2\ ^3F_3$	235 598	$5d5f\ ^3F^\circ_4$	−0.50	1.12(10)
43.6277	13 741.5	$5d^2\ ^1D_2$	242 953	$5d5f\ ^3P^\circ_2$	−0.58	9.20(09)
43.6880	13 741.5	$5d^2\ ^1D_2$	242 636	$5d5f\ ^1F^\circ_3$	−0.72	6.66(09)
43.7250	0.0	$5d^2\ ^3F_2$	228 702	$5d5f\ ^3F^\circ_2$	−0.01	3.40(10)
43.8408	11 519.4	$5d^2\ ^3F_4$	239 614	$5d5f\ ^3G^\circ_5$	0.70	1.75(11)
43.8714	11 519.4	$5d^2\ ^3F_4$	239 456	$5d5f\ ^3D^\circ_3$	−0.58	9.04(09)
43.9991	16 330.6	$5d^2\ ^3P_1$	243 609	$5d5f\ ^3P^\circ_1$	−0.23	2.03(10)
44.1074	11 519.4	$5d^2\ ^3F_4$	238 239	$5d5f\ ^3G^\circ_4$	0.03	3.66(10)
44.1257	16 330.6	$5d^2\ ^3P_1$	242 953	$5d5f\ ^3P^\circ_2$	−0.97	3.68(09)
44.2547	6244.7	$5d^2\ ^3F_3$	232 210	$5d5f\ ^3G^\circ_3$	−0.22	2.07(10)
44.3030	13 741.5	$5d^2\ ^1D_2$	239 456	$5d5f\ ^3D^\circ_3$	0.29	6.67(10)
44.4474	13 741.5	$5d^2\ ^1D_2$	238 727	$5d5f\ ^3D^\circ_2$	−0.40	1.36(10)
44.4854	22 345.8	$5d^2\ ^1G_4$	247 139	$5d5f\ ^1H^\circ_5$	0.79	2.07(11)
44.6272	11 519.4	$5d^2\ ^3F_4$	235 598	$5d5f\ ^3F^\circ_4$	−0.38	1.40(10)
44.7173	6244.7	$5d^2\ ^3F_3$	229 873	$5d5f\ ^3F^\circ_3$	−0.37	1.43(10)
44.7989	12 838.7	$5d^2\ ^3P_0$	236 062	$5d5f\ ^3D^\circ_1$	−0.05	2.99(10)
44.8505	6244.7	$5d^2\ ^3F_3$	229 205	$5d5f\ ^3H^\circ_4$	0.11	4.27(10)
44.9649	16 330.6	$5d^2\ ^3P_1$	238 727	$5d5f\ ^3D^\circ_2$	−0.11	2.59(10)
45.1889	6244.7	$5d^2\ ^3F_3$	227 536	$5d5f\ ^1G^\circ_4$	−0.79	5.34(09)
45.2501	22 615.4	$5d^2\ ^3P_2$	243 609	$5d5f\ ^3P^\circ_1$	−0.67	6.89(09)
45.3854	22 615.4	$5d^2\ ^3P_2$	242 953	$5d5f\ ^3P^\circ_2$	0.12	4.22(10)
45.3947	22 345.8	$5d^2\ ^1G_4$	242 636	$5d5f\ ^1F^\circ_3$	−0.90	4.11(09)
45.4415	13 741.5	$5d^2\ ^1D_2$	233 804	$5d5f\ ^1D^\circ_2$	−0.19	2.07(10)
45.4502	22 615.4	$5d^2\ ^3P_2$	242 636	$5d5f\ ^1F^\circ_3$	0.43	8.59(10)
45.5099	16 330.6	$5d^2\ ^3P_1$	236 062	$5d5f\ ^3D^\circ_1$	−0.95	3.65(09)
45.5408	11 519.4	$5d^2\ ^3F_4$	231 099	$5d5f\ ^3H^\circ_5$	−0.14	2.33(10)
45.7733	13 741.5	$5d^2\ ^1D_2$	232 210	$5d5f\ ^3G^\circ_3$	−0.44	1.16(10)
45.9385	11 519.4	$5d^2\ ^3F_4$	229 205	$5d5f\ ^3H^\circ_4$	−0.81	4.92(09)
45.9830	16 330.6	$5d^2\ ^3P_1$	233 804	$5d5f\ ^1D^\circ_2$	−0.06	2.73(10)
46.0268	22 345.8	$5d^2\ ^1G_4$	239 614	$5d5f\ ^3G^\circ_5$	−0.80	5.02(09)
46.2692	13 741.5	$5d^2\ ^1D_2$	229 873	$5d5f\ ^3F^\circ_3$	−0.34	1.41(10)
46.2724[b]	22 615.4	$5d^2\ ^3P_2$	238 727	$5d5f\ ^3D^\circ_2$	−0.69	6.44(09)
46.2933	11 519.4	$5d^2\ ^3F_4$	227 536	$5d5f\ ^1G^\circ_4$	−0.62	7.49(09)
46.8937	22 345.8	$5d^2\ ^1G_4$	235 598	$5d5f\ ^3F^\circ_4$	−0.13	2.25(10)
47.6906	43 110.1	$5d^2\ ^1S_0$	252 797	$5d7p\ ^3D^\circ_1$	−0.83	4.35(09)
47.9044	22 345.8	$5d^2\ ^1G_4$	231 099	$5d5f\ ^3H^\circ_5$	−0.73	5.45(09)
48.6138	43 110.1	$5d^2\ ^1S_0$	248 815	$5d5f\ ^1P^\circ_1$	−0.18	1.85(10)
48.7347	22 345.8	$5d^2\ ^1G_4$	227 536	$5d5f\ ^1G^\circ_4$	−0.52	8.56(09)
56.8647	72 958.7	$5d6s\ ^1D_2$	248 815	$5d5f\ ^1P^\circ_1$	−0.96	2.26(09)
58.1049[b]	43 110.1	$5d^2\ ^1S_0$	215 212.7	$6s6p\ ^1P^\circ_1$	−0.96	2.17(09)
70.2963	72 958.7	$5d6s\ ^1D_2$	215 212.7	$6s6p\ ^1P^\circ_1$	0.01	1.38(10)
72.3876	6244.7	$5d^2\ ^3F_3$	144 389.9	$5d6p\ ^3P^\circ_2$	−0.99	1.29(09)
72.5616	60 295.5	$5d6s\ ^3D_2$	198 108.2	$6s6p\ ^3P^\circ_2$	−0.60	3.17(09)
72.6162	0.0	$5d^2\ ^3F_2$	137 709.3	$5d6p\ ^3P^\circ_1$	−0.86	1.75(09)
74.4887	11 519.4	$5d^2\ ^3F_4$	145 767.9	$5d6p\ ^1F^\circ_3$	−0.76	2.10(09)
76.0740	66 657.7	$5d6s\ ^3D_3$	198 108.2	$6s6p\ ^3P^\circ_2$	0.17	1.71(10)
76.1103	11 519.4	$5d^2\ ^3F_4$	142 907.9	$5d6p\ ^3F^\circ_4$	0.02	1.20(10)

Table 7. (Continued.)

	Lower level[a]		Upper level[a]			
λ^a(nm)	E (cm^{-1})	Designation	E (cm^{-1})	Designation	log gf^c	$gA^c(s^{-1})$
78.0884	16 330.6	$5d^2\ ^3P_1$	144 389.9	$5d6p\ ^3P^\circ_2$	−0.85	1.54(09)
78.5897	58 514.2	$5d6s\ ^3D_1$	185 757.2	$6s6p\ ^3P^\circ_1$	−0.59	2.76(09)
78.6254	6244.7	$5d^2\ ^3F_3$	133 430.0	$5d6p\ ^1D^\circ_2$	−0.08	9.09(09)
79.0235[b]	22 615.4	$5d^2\ ^3P_2$	149 160.1	$5d6p\ ^1P^\circ_1$	−0.53	3.13(09)
79.7057	60 295.5	$5d6s\ ^3D_2$	185 757.2	$6s6p\ ^3P^\circ_1$	−0.11	8.19(09)
79.7645	11 519.4	$5d^2\ ^3F_4$	136 887.8	$5d6p\ ^3D^\circ_3$	0.25	1.88(10)
80.0832	12 838.7	$5d^2\ ^3P_0$	137 709.3	$5d6p\ ^3P^\circ_1$	−0.97	1.12(09)
80.6659	13 741.5	$5d^2\ ^1D_2$	137 709.3	$5d6p\ ^3P^\circ_1$	−0.46	3.58(09)
80.9569	58 514.2	$5d6s\ ^3D_1$	182 036.7	$6s6p\ ^3P^\circ_0$	−0.46	3.57(09)
81.0225	22 345.8	$5d^2\ ^1G_4$	145 767.9	$5d6p\ ^1F^\circ_3$	0.44	2.78(10)
81.1460	6244.7	$5d^2\ ^3F_3$	129 479.5	$5d6p\ ^3F^\circ_3$	−0.08	8.45(09)
81.3528	16 330.6	$5d^2\ ^3P_1$	139 252.1	$5d6p\ ^3P^\circ_0$	−0.58	2.68(09)
81.4653	6244.7	$5d^2\ ^3F_3$	128 997.1	$5d6p\ ^3D^\circ_2$	−0.20	6.39(09)
81.7492	0.0	$5d^2\ ^3F_2$	122 325.8	$5d6p\ ^3D^\circ_1$	−0.11	7.77(09)
82.1188	22 615.4	$5d^2\ ^3P_2$	144 389.9	$5d6p\ ^3P^\circ_2$	0.08	1.19(10)
82.3875	16 330.6	$5d^2\ ^3P_1$	137 709.3	$5d6p\ ^3P^\circ_1$	−0.67	2.09(09)
83.5501	13 741.5	$5d^2\ ^1D_2$	133 430.0	$5d6p\ ^1D^\circ_2$	−0.23	5.58(09)
84.2733	0.0	$5d^2\ ^3F_2$	118 662.8	$5d6p\ ^3F^\circ_2$	−0.13	7.07(09)
84.7749	11 519.4	$5d^2\ ^3F_4$	129 479.5	$5d6p\ ^3F^\circ_3$	−0.45	3.26(09)
86.7633	13 741.5	$5d^2\ ^1D_2$	128 997.1	$5d6p\ ^3D^\circ_2$	−0.25	4.98(09)
87.3045	22 345.8	$5d^2\ ^1G_4$	136 887.8	$5d6p\ ^3D^\circ_3$	−0.55	2.44(09)
87.5102	22 615.4	$5d^2\ ^3P_2$	136 887.8	$5d6p\ ^3D^\circ_3$	−0.95	9.79(08)
88.7567	16 330.6	$5d^2\ ^3P_1$	128 997.1	$5d6p\ ^3D^\circ_2$	−0.52	2.58(09)
91.3347	12 838.7	$5d^2\ ^3P_0$	122 325.8	$5d6p\ ^3D^\circ_1$	−0.77	1.34(09)
93.3410	22 345.8	$5d^2\ ^1G_4$	129 479.5	$5d6p\ ^3F^\circ_3$	−0.84	1.11(09)
94.2961	43 110.1	$5d^2\ ^1S_0$	149 160.1	$5d6p\ ^1P^\circ_1$	−0.61	1.86(09)
95.3096	13 741.5	$5d^2\ ^1D_2$	118 662.8	$5d6p\ ^3F^\circ_2$	−0.87	9.85(08)
118.9151	60 295.5	$5d6s\ ^3D_2$	144 389.9	$5d6p\ ^3P^\circ_2$	−0.48	1.58(09)
123.8574	58 514.2	$5d6s\ ^3D_1$	139 252.1	$5d6p\ ^3P^\circ_0$	−0.47	1.49(09)
126.2707	58 514.2	$5d6s\ ^3D_1$	137 709.3	$5d6p\ ^3P^\circ_1$	−0.13	3.11(09)
126.4066	66 657.7	$5d6s\ ^3D_3$	145 767.9	$5d6p\ ^1F^\circ_3$	−0.07	3.60(09)
128.6456	66 657.7	$5d6s\ ^3D_3$	144 389.9	$5d6p\ ^3P^\circ_2$	−0.18	2.70(09)
129.1759	60 295.5	$5d6s\ ^3D_2$	137 709.3	$5d6p\ ^3P^\circ_1$	−0.58	1.06(09)
130.5611	60 295.5	$5d6s\ ^3D_2$	136 887.8	$5d6p\ ^3D^\circ_3$	0.29	7.58(09)
131.1465	66 657.7	$5d6s\ ^3D_3$	142 907.9	$5d6p\ ^3F^\circ_4$	0.52	1.27(10)
131.2319	72 958.7	$5d6s\ ^1D_2$	149 160.1	$5d6p\ ^1P^\circ_1$	−0.04	3.54(09)
133.4841	58 514.2	$5d6s\ ^3D_1$	133 430.0	$5d6p\ ^1D^\circ_2$	−0.01	3.67(09)
136.7341	60 295.5	$5d6s\ ^3D_2$	133 430.0	$5d6p\ ^1D^\circ_2$	−0.26	1.95(09)
137.3439	72 958.7	$5d6s\ ^1D_2$	145 767.9	$5d6p\ ^1F^\circ_3$	0.20	5.61(09)
139.9933	72 958.7	$5d6s\ ^1D_2$	144 389.9	$5d6p\ ^3P^\circ_2$	−0.19	2.23(09)
142.3889	66 657.7	$5d6s\ ^3D_3$	136 887.8	$5d6p\ ^3D^\circ_3$	−0.32	1.57(09)
144.5413	60 295.5	$5d6s\ ^3D_2$	129 479.5	$5d6p\ ^3F^\circ_3$	−0.27	1.72(09)
145.5559	60 295.5	$5d6s\ ^3D_2$	128 997.1	$5d6p\ ^3D^\circ_2$	−0.77	5.32(08)
156.7095	58 514.2	$5d6s\ ^3D_1$	122 325.8	$5d6p\ ^3D^\circ_1$	−0.47	9.05(08)
159.1804	66 657.7	$5d6s\ ^3D_3$	129 479.5	$5d6p\ ^3F^\circ_3$	0.05	2.93(09)
160.4126	66 657.7	$5d6s\ ^3D_3$	128 997.1	$5d6p\ ^3D^\circ_2$	−0.07	2.22(09)
161.2132	60 295.5	$5d6s\ ^3D_2$	122 325.8	$5d6p\ ^3D^\circ_1$	−0.26	1.41(09)
165.3662	72 958.7	$5d6s\ ^1D_2$	133 430.0	$5d6p\ ^1D^\circ_2$	−0.72	4.62(08)
166.2540	58 514.2	$5d6s\ ^3D_1$	118 662.8	$5d6p\ ^3F^\circ_2$	−0.18	1.61(09)
171.3270	60 295.5	$5d6s\ ^3D_2$	118 662.8	$5d6p\ ^3F^\circ_2$	−0.21	1.41(09)
176.9249	72 958.7	$5d6s\ ^1D_2$	129 479.5	$5d6p\ ^3F^\circ_3$	−0.34	9.71(08)
178.4499	72 958.7	$5d6s\ ^1D_2$	128 997.1	$5d6p\ ^3D^\circ_2$	−0.37	9.02(08)

[a] From Kramida and Shirai (2009).
[b] Wavelengths deduced from available experimental energy values.
[c] This work (HFR+CPOL).

Table 8. Transition probabilities for forbidden lines in W V. Only transitions for which A-values are greater than 2 s^{-1} and λ are shorter than 2000 nm are listed. A(B) is written for A × 10^B.

	Lower level[b]		Upper level[b]			
λ[a](nm)	E (cm^{-1})	Designation	E (cm^{-1})	Designation	Type	A^c_{ki}(s^{-1})
137.0638	0.0	$5d^2\ ^3F_2$	72 958.7	$5d6s\ ^1D_2$	M1+E2	2.11(+0)
149.8936	6244.7	$5d^2\ ^3F_3$	72 958.7	$5d6s\ ^1D_2$	M1+E2	5.79(+1)
150.0202	0.0	$5d^2\ ^3F_2$	66 657.7	$5d6s\ ^3D_3$	M1+E2	9.83(+0)
162.7623	11 519.4	$5d^2\ ^3F_4$	72 958.7	$5d6s\ ^1D_2$	E2	2.50(+1)
165.5273	6244.7	$5d^2\ ^3F_3$	66 657.7	$5d6s\ ^3D_3$	E2	1.40(+2)
165.8499	0.0	$5d^2\ ^3F_2$	60 295.5	$5d6s\ ^3D_2$	E2	2.21(+2)
168.8699	13 741.5	$5d^2\ ^1D_2$	72 958.7	$5d6s\ ^1D_2$	M1+E2	1.21(+2)
170.8987	0.0	$5d^2\ ^3F_2$	58 514.2	$5d6s\ ^3D_1$	E2	3.12(+2)
176.5908	16 330.6	$5d^2\ ^3P_1$	72 958.7	$5d6s\ ^1D_2$	M1+E2	2.43(+0)
181.3621	11 519.4	$5d^2\ ^3F_4$	66 657.7	$5d6s\ ^3D_3$	E2	2.89(+2)
185.0111	6244.7	$5d^2\ ^3F_3$	60 295.5	$5d6s\ ^3D_2$	M1+E2	1.69(+2)
188.9780	13 741.5	$5d^2\ ^1D_2$	66 657.7	$5d6s\ ^3D_3$	M1+E2	4.38(+1)
191.3162	6244.7	$5d^2\ ^3F_3$	58 514.2	$5d6s\ ^3D_1$	E2	1.05(+2)
197.5781	22 345.8	$5d^2\ ^1G_4$	72 958.7	$5d6s\ ^1D_2$	E2	3.52(+2)
198.6362	22 615.4	$5d^2\ ^3P_2$	72 958.7	$5d6s\ ^1D_2$	M1+E2	7.05(+1)
198.7001	16 330.6	$5d^2\ ^3P_1$	66 657.7	$5d6s\ ^3D_3$	E2	3.77(+1)
204.9527	11 519.4	$5d^2\ ^3F_4$	60 295.5	$5d6s\ ^3D_2$	E2	6.46(+1)
210.6512	12 838.7	$5d^2\ ^3P_0$	60 295.5	$5d6s\ ^3D_2$	E2	2.87(+1)
214.7367	13 741.5	$5d^2\ ^1D_2$	60 295.5	$5d6s\ ^3D_2$	M1+E2	1.60(+1)
223.2810	13 741.5	$5d^2\ ^1D_2$	58 514.2	$5d6s\ ^3D_1$	M1+E2	2.72(+1)
225.6031	22 345.8	$5d^2\ ^1G_4$	66 657.7	$5d6s\ ^3D_3$	E2	9.47(+0)
226.9843	22 615.4	$5d^2\ ^3P_2$	66 657.7	$5d6s\ ^3D_3$	M1+E2	2.31(+1)
227.3839	16 330.6	$5d^2\ ^3P_1$	60 295.5	$5d6s\ ^3D_2$	M1+E2	4.27(+0)
231.8930	0.0	$5d^2\ ^3F_2$	43 110.1	$5d^2\ ^1S_0$	E2	2.73(+0)
236.9866	16 330.6	$5d^2\ ^3P_1$	58 514.2	$5d6s\ ^3D_1$	E2	3.49(+1)
263.4282	22 345.8	$5d^2\ ^1G_4$	60 295.5	$5d6s\ ^3D_2$	E2	4.45(+0)
265.3131	22 615.4	$5d^2\ ^3P_2$	60 295.5	$5d6s\ ^3D_2$	M1+E2	6.80(+0)
334.9278	43 110.1	$5d^2\ ^1S_0$	72 958.7	$5d6s\ ^1D_2$	E2	3.31(+0)
340.4020	13 741.5	$5d^2\ ^1D_2$	43 110.1	$5d^2\ ^1S_0$	E2	1.09(+1)
373.3138	16 330.6	$5d^2\ ^3P_1$	43 110.1	$5d^2\ ^1S_0$	M1	6.90(+1)
610.6784	6244.7	$5d^2\ ^3F_3$	22 615.4	$5d^2\ ^3P_2$	M1+E2	2.72(+0)
620.9038	6244.7	$5d^2\ ^3F_3$	22 345.8	$5d^2\ ^1G_4$	M1+E2	7.58(+0)
692.1141	58 514.2	$5d6s\ ^3D_1$	72 958.7	$5d6s\ ^1D_2$	M1+E2	8.25(+0)
727.5221	0.0	$5d^2\ ^3F_2$	13 741.5	$5d^2\ ^1D_2$	M1+E2	5.51(+0)
923.4147	11 519.4	$5d^2\ ^3F_4$	22 345.8	$5d^2\ ^1G_4$	M1+E2	3.54(+0)
1126.5917	13 741.5	$5d^2\ ^1D_2$	22 615.4	$5d^2\ ^3P_2$	M1	7.05(+0)
1571.3540	60 295.5	$5d6s\ ^3D_2$	66 657.7	$5d6s\ ^3D_3$	M1	4.03(+0)
1590.7059	16 330.6	$5d^2\ ^3P_1$	22 615.4	$5d^2\ ^3P_2$	M1	2.16(+0)
1600.9206	0.0	$5d^2\ ^3F_2$	6244.7	$5d^2\ ^3F_3$	M1	5.60(+0)
1895.3249	6244.7	$5d^2\ ^3F_3$	11 519.4	$5d^2\ ^3F_4$	M1	2.65(+0)

[a] Vacuum wavelengths (below 200 nm) and air wavelengths (above 200 nm) deduced from the experimental levels.
[b] From Kramida and Shirai (2009).
[c] This work (HFR+CPOL).

4. Conclusion

Atomic structure and radiative rate calculations were performed in Yb-like tungsten using several semi-empirical and *ab initio* methods. From detailed comparisons between these different approaches, the accuracy of the computed transition probabilities and oscillator strengths has been estimated. It has been shown that some line strengths are particularly sensitive to level mixings which are expected to be better estimated when using semi-empirical methods. The new set of radiative data reported in this paper for allowed and forbidden lines in W V should be useful for plasma diagnostics in future fusion reactors where tungsten will be used as plasma-facing material.

Acknowledgments

EB, PQ and PP are respectively Research Director, Senior Research Associate and Research Associate of the Belgian FRS-FNRS. Financial support from this organization and from ADAS-EU is acknowledged. SEY was financially supported by a grant from the FRS-FNRS (2011/V 6/5/013-IB/JN-1343) and from the Marien Ngouabi University (Congo). He is grateful to Belgian colleagues for their hospitality during his stay at Mons University.

References

Churilov S S, Kildiyarova R R and Joshi Y N 1996 *Can. J. Phys.* **74** 145

Cowan R D 1981 *The Theory of Atomic Structure and Spectra* (Berkeley, CA: University of California Press)

Dyall K G, Grant I P, Johnson C T, Parpia F A and Plummer E P 1989 *Comput. Phys. Commun.* **55** 425

Enzonga Yoca S, Quinet P and Biémont É 2012a *J. Phys. B: At. Mol. Opt. Phys.* **45** 035001

Enzonga Yoca S, Palmeri P, Quinet P, Jumet G and Biémont É 2012b *J. Phys. B: At. Mol. Opt. Phys.* **45** 035002

Federici G *et al* 2001 *Nucl. Fusion* **41** 1967

Fraga S, Karwowski J and Saxena K M S 1976 *Handbook of Atomic Data* (Amsterdam: Elsevier)

Fullerton L W and Rinker G A 1976 *Phys. Rev.* A **13** 1283

Grant I P and McKenzie B J 1980 *J. Phys. B: At. Mol. Phys.* **13** 2671

Grant I P, McKenzie B J, Norrington P H, Mayers D F and Pyper N C 1980 *Comput. Phys. Commun.* **21** 207

Gu M F 2003 *Astrophys. J.* **582** 1241

Kildiyarova R R, Churilov S S, Joshi Y N and Ryabtsev A N 1996 *Phys. Scr.* **53** 454

Kramida A E and Shirai T 2009 *At. Data Nucl. Data Tables* **95** 305

Malcheva G, Enzonga Yoca S, Mayo R, Ortiz M, Engström L, Lundberg H, Nilsson H, Biémont É and Blagoev K 2009 *Mon. Not. R. Astron. Soc.* **396** 2289

McKenzie B J, Grant I P and Norrington P H 1980 *Comput. Phys. Commun.* **21** 233

Meijer F G 1986 *Physica* **141C** 230

Mohr P J 1974 *Ann. Phys.* **88** 52

Mohr P J 1975 *Phys. Rev. Lett.* **34** 1050

Neu R *et al* 2005 *Nucl. Fusion* **45** 209

Nilsson H, Engström L, Lundberg H, Palmeri P, Fivet V, Quinet P and Biémont É 2008 *Eur. Phys. J.* D **49** 13

Norrington P H 2009 http://www.am.qub.ac.uk/DARC/

Palmeri P, Quinet P, Fivet V, Biémont É, Nilsson H, Engström L and Lundberg H 2008 *Phys. Scr.* **78** 015304

Pospieszczyk A 2006 *Nuclear Fusion Research* (Berlin: Springer)

Quinet P, Palmeri P and Biémont É 2011 *J. Phys. B : At. Mol. Opt. Phys.* **44** 145005

Quinet P, Palmeri P, Biémont É, McCurdy M M, Rieger G, Pinnington E H, Wickliffe M E and Lawler J E 1999 *Mon. Not. R. Astr. Soc.* **307** 934

Quinet P, Vinogradoff V, Palmeri P and Biémont É 2010 *J. Phys. B: At. Mol. Opt. Phys.* **43** 144003

Safronova U I and Safronova A S 2010 *J. Phys. B: At. Mol. Opt. Phys.* **43** 074026

Skinner C H 2008 *Can. J. Phys.* **86** 285

Skinner C H 2009 *Phys. Scr.* T **134** 014022

Uehling E A 1935 *Phys. Rev.* **48** 55